

Vehicle-to-Vehicle Communications for AVCS Platooning

Tushar Tank and Jean-Paul M. G. Linnartz

Abstract—Vehicle-to-vehicle radio links suffer from multipath fading and interference from other vehicles. We discuss the impact of these effects on communication networks supporting an intelligent transportation system (ITS), in particular, automated vehicle control systems (AVCS's). A statistical model for this channel is considered, and the performance of the network involving many links is evaluated. We compare the performance of time division multiple access (TDMA), direct-sequence code division multiple access (DS-CDMA), and frequency hopping with TDMA in this environment. Reliability of the radio link is investigated by specifying the radio spectrum occupation for a given required reliability of the radio link.

Index Terms—Automated highways, land mobile radio data communication, multiple-access communication, Rician channels.

I. INTRODUCTION

RECENTLY, implementation of advanced communication technology has been propounded as a method to improve the efficiency and safety of ground transportation. Projects such as Road Automobile Communication Systems (RACS) in Japan [1], PROMETHEUS in Europe [2], and Partners for Advanced Transit and Highway (PATH) in the United States are currently engaged in the design of such systems called intelligent transportation systems (ITS's) in Japan and the United States and road transport informatics (RTI) in Europe. These projects encompass automated vehicle control systems (AVCS's), advanced traffic management and information system (ATMIS), advanced vehicle identification (AVI), and advanced driver information system (ADIS) as platforms from which ITS can be realized. Many see these projects as a means of improving safety and efficiency of the highway system, which, in turn, would lead to an increase in the productivity of commuters as well as alleviate pollution [3].

Vehicle-to-vehicle communication is of critical importance to such ITS projects, especially in AVCS employing platoons [4]. Although communication occurs only over a relatively short range, from less than 1 m to tens of meters, the communication links have to be extremely reliable, despite the

presence of multipath reflections and interference from other links using the same frequency channel.

In [5] and [6], a vehicle-to-basestation Rayleigh fading channel has been investigated, whereas in [7] and [8], a vehicle-to-vehicle Rayleigh fading channel has been investigated. However, in this report, we extend these models, to best represent a vehicle-to-vehicle channel in an ITS setting, by considering a Rician fading channel with a direct line-of-sight (LOS) component and a strong ground-reflected component in a mobile-to-mobile environment.

In order to combat the effects of multipath fading and associated Doppler shift as well as interference from other links, multiple-access schemes such as time division multiple access (TDMA), direct-sequence code division multiple access (DS-CDMA), and frequency hopping with TDMA are investigated. [4] and [9] have shown that message delays within a platoon environment can have dire consequences. Thus, the performance of these various multiple-access schemes is quantified by packet erasure rates (PER's) as well as reliability (probability of a successful message reception in a fixed time interval) for a given spectral allocation. Network protocol and frequency reuse in a platoon scenario will also be discussed.

This paper is organized as follows. We begin in Section II by discussing the platoon model in which the communication links are located and highlight various elements that will affect the channel and communication link. In Section III, the channel model is described. Sections IV and V deal with the modulation and multiple-access schemes that are implemented in this channel. Section VI discusses network protocol and frequency-sharing procedures. In Section VII, we formulate numerical results of the issues discussed in the preceding sections. Section VIII summarizes these results and draws conclusions and recommendations of this study.

II. PLATOON MODEL

In [4], a method of efficient vehicle control by grouping vehicles in platoons has been proposed.

“It requires electronically linked cars to travel in instrumented lanes with facilities to allow the vehicles to join and exit platoons smoothly at highway speeds. Estimates suggest that a single automated lane could carry as much traffic as three or four ordinary lanes. Platoons of up to four cars at speeds of 55 m.p.h. and up have already been tested and plans to test platoons of up to 20 cars are being implemented. It is possible to obtain very accurate lane holding (within 15 cm when under a variety of anomalous

Manuscript received August 25, 1995; revised March 21, 1996. This work was supported in part by the State of California Business, Transportation and Housing Agency, Department of Transportation, and Partners in Advanced Transit and Highways (PATH) program.

T. Tank is with the Department of Electrical Engineering and Computing Science, University of California, Berkeley, CA 94720-1770 USA and C-Cube Microsystems, Milpitas, CA 95035 USA.

J.-P. M. G. Linnartz is with the Department of Electrical Engineering and Computer Science, University of California, Berkeley, CA 94720-1770 USA and Philips Research, Natuurkundig Laboratorium WY 8, Holstlaan, 5656 AA Eindhoven, The Netherlands.

Publisher Item Identifier S 0018-9545(97)03113-7.

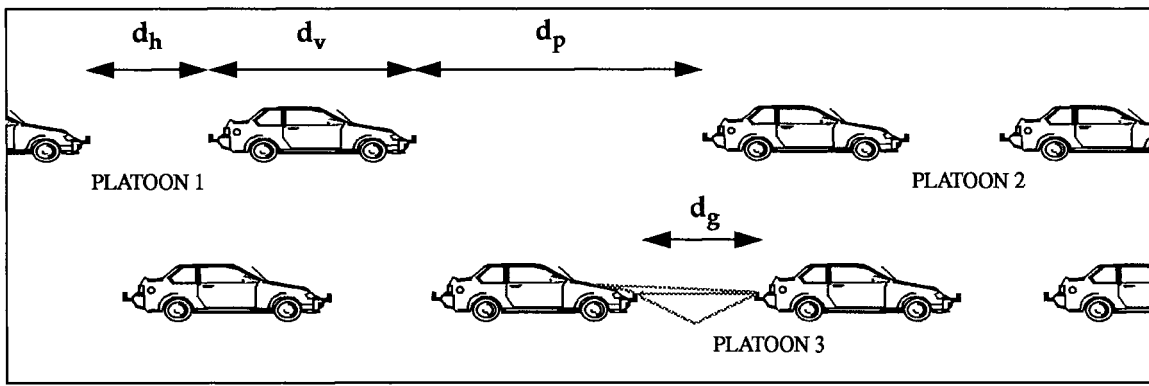


Fig. 1. Platoon model.

conditions) while maintaining excellent ride quality. Highway lanes could be much narrower once automated. High-precision vehicle-follower control appears possible when dynamic data obtained by ranging sensors are combined with communication between cars” [3].

We consider AVCS in a platoon environment, where a platoon consists of N vehicles. As depicted in Fig. 1, the distance between vehicles is denoted as d_h and is on the order of 1 or 2 m [4]. The vehicle length, platoon-following distance, and lane width are denoted as d_v , d_p , and d_l , respectively, while the communication link under study is denoted as d_g .

In slotted-access cellular mobile transmission schemes, different cells transmit over different frequencies in order to reduce interference. Frequency bands can be reused in cells spaced far enough apart such that the interfering energy between these cells is negligible. Each platoon, including the distance between the platoons, d_p , is considered a cell. Unlike most cellular radio schemes, the cells here are in relative motion with each other, since platoons in either lane may have a net difference in velocities. Thus, we define two frequency reuse distances, d_r and d_s . The distance d_r is the reuse distance within a lane, whereas d_s is the reuse distance between lanes.

Thus, for TDMA, if a cluster of C different frequencies is used, the frequency reuse distance within a lane is

$$d_r = C_r(d_p + (N - 1)(d_v + d_h)) \quad (1)$$

whereas the reuse distance between lanes for both TDMA and CDMA is

$$d_s = C_s d_l. \quad (2)$$

Thus, for TDMA, $C = C_r C_s$ radio channels are required, each with bandwidth B_T . Messages are of relatively short duration, typically a few hundreds of bits. The required transmission bandwidth is determined by the cycle duration T_C during which all vehicles in a platoon transmit their speed and acceleration data. Since CDMA transmission suppresses interference, successive platoons and platoons in other lanes may use the same channel.

III. RADIO CHANNEL NETWORK MODEL

Vehicle-to-vehicle data communication will mainly consist of the continuous (routine) exchange of telemetric data, such

as vehicle status, speed, and acceleration. Interfering signals will be present from vehicles within the platoon and from outside the platoon (from vehicles in other lanes). Vehicles with bumper-mounted directional antennas are considered.

We model the vehicle-to-vehicle radio link statistically as a Rician fading channel. The dominant component in our Rician fading channel is likely to be relatively strong compared to the reflected signal (large Rician K factor), and the delay spread is likely to be relatively small because reflections occur in the immediate vicinity of the transmitter and receiver antenna [10]. We model the propagation channel as a dominant component consisting of a direct LOS wave and a ground-reflected wave, a set of early reflected waves, and intersymbol interference (ISI) caused by excessively delayed waves.

Propagation models proposed for microcellular communication model path loss, with a transition from free-space propagation to ground-wave propagation if $d_g \lambda < 4h_r h_t$, where d_g is the distance of the radio link under study, h_r and h_t are the heights of the receiving and transmitting antenna, respectively, and λ is the wavelength of the transmitted wave. Various models have been proposed, e.g., a step-wise transition from 20 to 40 log d at a certain (turnover) distance d_t . In [11], a smooth transition is suggested, with

$$\bar{p} = d_t^{-\beta_1} \left(1 + \frac{d_g}{d_t} \right)^{-\beta_2} \quad (3)$$

again, where d_t is the turnover distance and $\beta_1 = \beta_2 = 2$. However, when the distance between the receiver and transmitter antenna is small and unobstructed, the direct LOS component and the ground-reflected component will cause strong fluctuations in the received signal power due to mutual interference between these two waves. Thus, the local-mean power of the dominant wave does not show a smooth transition between free-space and ground-wave propagation. Rather, this transition is marked by strong fluctuations in the local-mean power.

The road surface is neither a perfect conductor nor dielectric, so the reflection coefficient depends on the dielectric constant $\epsilon = \epsilon_0 \epsilon_r$ and the conductivity σ of the road surface. In order to facilitate computation, we assume the road surface to be smooth and, thus, the dielectric constant and conductivity do not vary with the distance. The reflection coefficient for

horizontally polarized waves is given by [12]

$$\Gamma = \frac{\sin \Theta - \sqrt{(\varepsilon_r - j\chi) - (\cos \Theta)^2}}{\sin \Theta + \sqrt{(\varepsilon_r - j\chi) - (\cos \Theta)^2}} \quad (4)$$

where ω is the angular frequency of the signal, ε_0 is the dielectric constant of free space, and Θ is the angle of incidence, which we assume to be equal to the angle of reflection, and

$$\chi = \frac{\sigma}{\omega \varepsilon_0} = \frac{18 \times 10^9 \sigma}{f}. \quad (5)$$

For vertical polarization, the reflection coefficient is given by [12]

$$\Gamma = \frac{(\varepsilon_r - j\chi) \sin \Theta - \sqrt{(\varepsilon_r - j\chi) - (\cos \Theta)^2}}{(\varepsilon_r - j\chi) \sin \Theta + \sqrt{(\varepsilon_r - j\chi) - (\cos \Theta)^2}}. \quad (6)$$

Since this reflection coefficient is complex, the reflected ground wave will differ in both amplitude and phase. The phase difference of the two paths is [13]

$$\Delta\varphi = \frac{2\pi}{\lambda} \left\{ \sqrt{d_g^2 + (h_t + h_r)^2} - \sqrt{d_g^2 + (h_t - h_r)^2} \right\}. \quad (7)$$

If the field strength at the receiving antenna due to the direct LOS wave is E_d , then the received field due to the sum of the direct LOS component and ground-reflected component is

$$E = E_d [1 + |\Gamma| \exp(j\angle\Gamma - j\Delta\varphi)]. \quad (8)$$

Taking the absolute value, we find that

$$|E| = |E_d| [1 + |\Gamma|^2 + 2|\Gamma| \cos(\angle\Gamma - j\Delta\varphi)]^{1/2} \quad (9)$$

and since the received power p_r is proportional to the square of the received energy, we have

$$p_r = |E_d|^2 [1 + |\Gamma|^2 + 2|\Gamma| \cos(\angle\Gamma - j\Delta\varphi)] \quad (10)$$

and

$$\frac{p_r}{p_t} = \left(\frac{\lambda}{4\pi d_g} \right)^2 G_t G_r [1 + |\Gamma|^2 + 2|\Gamma| \cos(\angle\Gamma - j\Delta\varphi)]. \quad (11)$$

If $d_g \gg h_t h_r$, the angle of incidence becomes small and the reflection coefficient $\Gamma \rightarrow -1$. Thus, (9) becomes

$$|E| = 2|E_d| \sin \frac{\Delta\varphi}{2}. \quad (12)$$

Then, using the small-angle approximation $\sin \Delta\varphi \approx \Delta\varphi$ and expressing $\Delta\varphi \approx \frac{4\pi h_t h_r}{\lambda d_g}$, both valid approximations for a sufficiently large separation distance, (11) can be expressed as

$$\frac{p_r}{p_t} = -G_t G_r \left(\frac{h_t h_r}{d_g^2} \right)^2. \quad (13)$$

So, for large separation distances, the local-mean power falls as an inverse fourth-power law. From this analysis and empirical values reported for path loss, we conclude that free-space loss dominates propagation between antennas of vehicles belonging to same platoon, where there is no LOS component ($d_i < N(d_v + d_h) \ll d_t$), and plane earth loss for interference signals propagating from one platoon to another, where the propagation distances are large. Therefore, the n th vehicle in

a platoon receives a normalized interference signal with power \bar{p}_m from the $m+n+1$ th (for $m = 1, 2, \dots, M$) vehicle given by

$$\bar{p}_m \approx m(d_v + d_h)^{-\beta_1} \quad (14)$$

and interference from two cochannel platoons, with normalized power \bar{p}_r , given by

$$\bar{p}_r \approx d_r^{-(\beta_1 + \beta_2)} d_t^{-\beta_2}, \quad (15)$$

In a dispersive Rician fading channel, energy arrives at the transmitter from reflections as well as a dominant wave, which we compute as the phasor sum of a direct LOS wave and a strong ground-reflected wave. Thus, the received signal of the i th vehicle is in the form

$$\begin{aligned} \nu_i(t) = & c_0 \cos(\omega_c t + \Phi_0 + \Psi_i(t)) \\ & + \sum_{k=1}^M c_k \cos(\omega_c t + \Phi_k + \Psi(t - T_k)) \end{aligned} \quad (16)$$

where the constant c_0 represents the amplitude of the dominant component, as found in (8), and Φ_0 represents the phase delay in the dominant component. The variables c_k , Φ_k , and T_k represent the amplitudes, phases, and delay times of the k th reflected wave ($k = 1, 2, \dots, M$). Digital phase modulation is incorporated in $\Psi_i(t)$. The reflections $\{k: T_k < T_b\}$ are assumed to add coherently to the dominant component and, along with the dominant component, make up the first resolvable Rician path. The remaining reflections cause ISI.

We define the Rician parameter K_1 as the ratio of the power \bar{p}_0 in the dominant component to the local-mean scattered power \bar{p}_1 in the first resolvable path. The Rician parameter K_2 is defined as the ratio of the power \bar{p}_0 in the dominant component to the excessively delayed local-mean scattered power \bar{p}_2 . The local-mean power \bar{p} is the sum of the power in the dominant component and the average powers in the scattered components ($\bar{p} = \bar{p}_0 + \bar{p}_1 + \bar{p}_2$). The Rician K factor, defined as the ratio of the power in the dominant component to the total scattered power, is

$$K = \left(\frac{1}{K_1} + \frac{1}{K_2} \right)^{-1}. \quad (17)$$

Since the local-mean power of the dominant component varies with distance, as shown in the previous section, the above Rician parameters, although not stated explicitly, are also functions of distance.

This channel behaves as a narrowband Rician fading channel with Rayleigh-distributed ISI. For $m = 0, 1$, or 2 and $K_0 = 1$

$$c_0^2 = 2\bar{p}_0 = \frac{2\bar{p}K}{1+K} \quad (18)$$

$$\bar{p}_m = \frac{\bar{p}K}{K_m(1+K)}. \quad (19)$$

In the following, K is assumed to be determined by the propagation environment and path length. The relative values of K_1 and K_2 are determined by the delay profile and

symbol rate. The probability distribution function of the signal amplitude, expressed in terms of the local-mean power $= p$ and the Rician K factor, becomes

$$f_\rho\langle\rho|\bar{p}, K\rangle = \frac{\rho(1+K)}{\bar{p}KK_1} e^{-K_1} \exp\left(-\frac{\rho^2(1+K)}{2\bar{p}KK_1}\right) \cdot I_0\left(\rho K_1 \sqrt{\frac{2(1+K)}{\bar{p}K}}\right) \quad (20)$$

where $I_0(\cdot)$ is the modified Bessel function of the first kind. Thus, for the instantaneous power we have

$$f_p\langle p|\bar{p}, K\rangle = f_\rho\langle\rho|\bar{p}, K\rangle \left| \frac{d\rho}{dp} \right| = \frac{(1+K)}{2\bar{p}KK_1} e^{-K_1} \exp\left(-\frac{p(1+K)}{\bar{p}KK_1}\right) \cdot I_0\left(2K_1 \sqrt{\frac{p(1+K)}{\bar{p}K}}\right). \quad (21)$$

For interfering signals, the propagation distance is significantly larger, and because of the relatively low antenna height, a LOS component may not be present. In such cases, Rayleigh fading (complex Gaussian) appears a reasonable model.

IV. MODULATION SCHEME

Ideally, the bit error rates (BER's) for BPSK modulation in a time-invariant, additive white Gaussian noise (AWGN) channel is [14]

$$P_b(e) = \frac{1}{2} \operatorname{erfc} \sqrt{\frac{E_b}{N_0}} \quad (22)$$

where N_0 is the (one-sided) spectral power density of the AWGN, E_b is the constant received energy per bit ($E_b = p_0 T_b$), and $\operatorname{erfc}(\cdot)$ denotes the complementary error function [15]. The in-phase component of Rayleigh fading cochannel interference may be approximated as Gaussian noise, giving a mean error probability of [16]

$$P_b(e|\rho, \bar{p}_r, \bar{p}_2) = \frac{1}{2} \operatorname{erfc} \left(\sqrt{\frac{\frac{1}{2}\rho^2 T_b}{\bar{p}_r T_b + \bar{p}_2 T_b + N_0}} \right). \quad (23)$$

For CDMA, the probability of bit error is often approximated as [17]

$$P_b(e|\rho, \bar{p}_t, \bar{p}_2) = \frac{1}{2} \operatorname{erfc} \left(\sqrt{\frac{\frac{1}{2}\rho^2 T_b}{\frac{(\bar{p}_t T_b + \bar{p}_2 T_b)}{C_s N} + N_0}} \right) \quad (24)$$

where N is the spreading gain of the CDMA scheme and C_s is the frequency reuse factor between lanes. The average BER can then be found by integrating over the Rician probability density function (pdf) of the signal amplitude given in (20)

$$\bar{p}_b = \int_0^\infty \frac{\rho(1+K)}{\bar{p}KK_1} e^{-K_1} \exp\left(-\frac{\rho^2(1+K)}{2\bar{p}KK_1}\right) \cdot I_0\left(\rho K_1 \sqrt{\frac{2(1+K)}{\bar{p}K}}\right) \times P_b\langle e|\rho, p_r, p_2\rangle d\rho. \quad (25)$$

V. MULTIPLE-ACCESS SCHEMES

In this section, we compare TDMA, TDMA with slow frequency-hopping interferers, and DS-CDMA with regards to PER's. We use spreading mainly to suppress interference. In other applications, the frequency diversity of CDMA is also exploited, however, as the delay spread is small [10], excessive bandwidth would be needed for our application. Dynamic power control cannot be easily used here with multiple receivers.

A packet erasure occurs when bit errors are in excess of the correcting capabilities of the error-correction coding being implemented. Slow and fast Rician fading of the wanted signal are considered with a block error-detection code that can correct up to M errors in a block of L bits.

With fast fading, the duration of the packets is substantially longer than the time constants of the multipath fading. This is the case with continuous-wave CDMA transmission, with a bit rate of 5 kb/s, a carrier frequency of 1 GHz, and a vehicle speed of 30m/s (~ 70 mi/h). The received signal experiences several fades during packet transmission. We assume that during 1-b time, the channel characteristics do not change, but that the received amplitudes are statistically independent from bit to bit, even though the receiver remains perfectly locked to the wanted signal. So, the probability of undetected packet errors for BPSK is obtained from

$$P\langle e|\bar{p}_0, \bar{p}_r\rangle = 1 - \sum_{m=0}^M \binom{L}{m} (1 - \bar{p}_b)^{L-m} (\bar{p}_b)^m \quad (26)$$

where the average bit error probability \bar{p}_b is expressed in (25).

Slow fading occurs when packets are of sufficiently short duration, that the received amplitude and carrier phase may be assumed to be constant throughout the duration of the packet. This condition is satisfied if the motion of the mobile terminal during the transmission time of a block of bits is negligible compared to the wavelength. This is the case with TDMA transmission at a channel rate above 100 kb/s to accommodate user bit rates of 5 kb/s with an average frame of 20 cars/platoons. The probability of packet erasure in a block of L bits with M -bit correction is found by averaging the probability of packet error over the Rician fading of the wanted signal [18]. In our case

$$P\langle e|\bar{p}_0, \bar{p}_t\rangle = \int_0^\infty \frac{(1+K)}{2\bar{p}KK_1} e^{-k_1} \exp\left(-\frac{p(1+K)}{\bar{p}KK_1}\right) \cdot I_0\left(2K_1 \sqrt{\frac{p(1+K)}{\bar{p}K}}\right) \left\{ 1 - \sum_{m=0}^M \binom{L}{m} \left(1 - \frac{1}{2} \operatorname{erfc} \left(\sqrt{\frac{pT_b}{\bar{p}_r T_b + \bar{p}_2 T_b + N_0}} \right) \right)^{L-m} \cdot \left(\frac{1}{2} \operatorname{erfc} \left(\sqrt{\frac{pT_b}{\bar{p}_r T_b + \bar{p}_2 T_b + N_0}} \right) \right)^m \right\} dp. \quad (27)$$

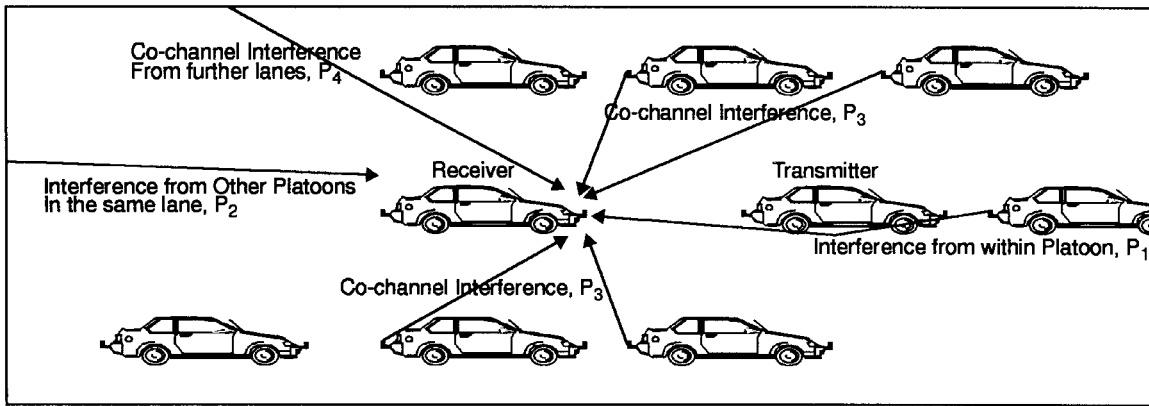


Fig. 2. Assumptions about interference in radio link.

VI. NETWORK PROTOCOL

Our TDMA radio protocol is as follows: the lead vehicle transmits a message containing speed and acceleration to the second vehicle. Upon reception of a report by the n -1th vehicle, the n th vehicle sends its report. The performance of the radio link can be quantified by the probability that a message can be successfully transmitted across a platoon from one vehicle to another. We define the completion of a message through a platoon in this manner as a cycle. If a vehicle does not recognize a message or erroneously detects a message, the cycle is interrupted. To ensure safe operation of the AVCS vehicle control system, we require a very small probability of undetected errors. On the other hand, we wish a large probability that a cycle is completed successfully. The n th vehicle transmits its report after it has successively received messages with a bit pattern that differed in less than M_2 places from a valid codeword of the n -1th vehicle. A message is assumed to be received successfully and reliably if the detected bit sequences do not differ in more than M_1 places from a valid code word. It is not necessary to take $M_1 = M_2$. In fact, if $M_1 < M_2$, the terminal may transmit its own status, assuming that its turn to transmit has arrived, yet not entirely relying upon the data in the received packet because of a large number of bit errors. The performance of the network is quantified by finding the probability that the n -1th vehicle successfully transmits its report to the n th vehicle, with $M_1 < M_2$. In an AVCS environment, the lead vehicle generates data that all vehicles in the platoon require [4], thus, we are also interested in the probability that the lead vehicle successfully transmits its report to the n th vehicle; this occurs if each hop has less than M_1 bit errors.

VII. NUMERICAL RESULTS

For our calculations, the length of each vehicle, d_v , was assumed to be 5 m, the lane width, d_l , was assumed to be 3 m, the distance between automated cars, d_h , was assumed to be 1 m, and the average velocity of an automated vehicle was assumed to be 70 mi/h. The distance of the radio link under study, d_g , was varied from 0.1 to 10 m [10]. From [10], we know that $K = 7$ db ($K_1 \approx 5$) is reasonable for most microcellular channels: we assume $K_1 = 10$ as an upper

bound. The signal-to-noise (AWGN Gaussian) ratio was set to 10 dB at $d_g = 1$ m and 30 dB at $d_g = 10$ m.

The radio link suffers from interference from within its platoon (P_1), from platoons in the same lane (P_2), and cochannel interference from platoons in other lanes (P_3 and P_4) (Fig. 2). In all simulations, we assume that the target vehicle is joining an infinitely long platoon. It should be noted that in TDMA transmission, each vehicle within a platoon is given a time slot in which to transmit, thus, P_1 will be zero, while for a CDMA-type transmission, all vehicles transmit at the same time, thus, P_1 must be taken into account. We assume P_2 is negligible since transmissions from other platoons must be reflected off vehicles, the road surface, and surroundings before reaching the receiver. These reflections will greatly attenuate the signal. We thus set $d_r = C_r = 0$ from (1). To obtain an upper bound on P_3 and P_4 , we assume that an infinitely long platoon would transmit as close as possible to the receiving vehicle. Preliminary measurements at the Richmond field station indicate that these signals attenuate by 10 dB for each land transversed, thus, P_4 would be 10 dB less than P_3 .

A. BER's

We will first show BER's as a function of distance as described in (23), (24), and (25) and compare them to a channel model in which a strongly reflected ground wave is not present. Fig. 3 examines the effect of varying the reuse pattern C_r for CDMA transmission employing horizontal or vertical polarization. For a spreading factor of $N = 32$, the BER's show a great change only when $C_r = 1$. For other curves (not plotted here), it appeared that for a reuse pattern greater than one or two and $N > 32$, the BER's remain relatively the same, independent of spreading factor and reuse pattern. We will concentrate on CDMA with a reuse factor $C_r = 2$ and a spreading factor $N = 32$, since this will give nearly the same performance as other schemes, but with minimal bandwidth.

The effects of varying frequency reuse patterns for TDMA is presented in Fig. 4. Here, we see that unlike the CDMA case, varying the reuse pattern has a significant impact on the BER's, thus, TDMA is more sensitive to interference than CDMA. However, as C_r and the bandwidth required increases, the

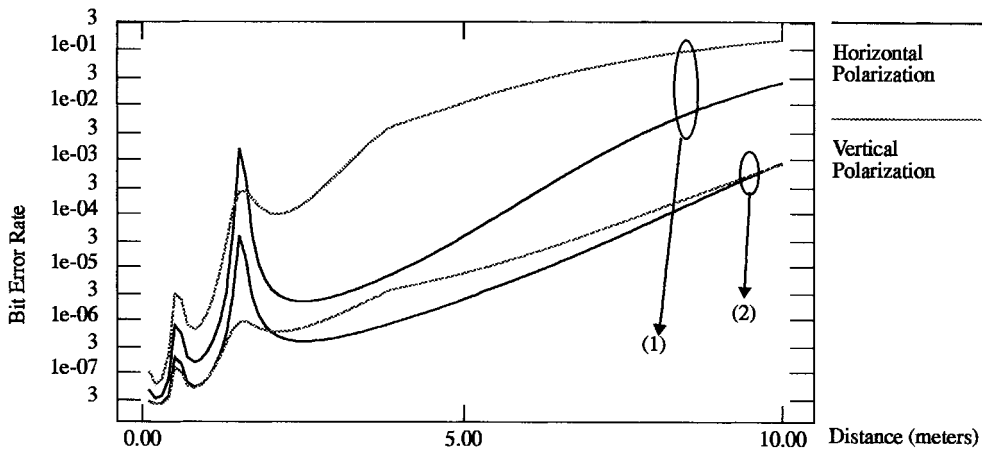


Fig. 3. BER's for CDMA $N = 32$ with vertical and horizontal polarization: (1) $C_r = 1$ and (2) $C_r = 2$.

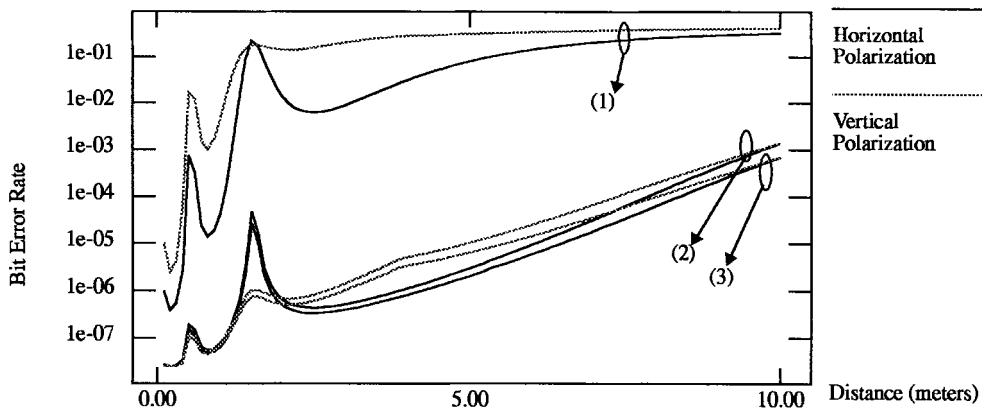


Fig. 4. BER's for TDMA with vertical and horizontal polarization: (1) $C_r = 1$, (2) $C_r = 2$, and (3) $C_r = 6$.

marginal return in performance decreases. We will concentrate on TDMA with a reuse pattern of $C_r = 3$.

B. BER's

As explained in Section V, we assume a fast fading channel for CDMA and a slow fading channel for TDMA. We also assume a packet length of $L = 76$ b with 1-b correction ($M_1 = 1$) [19]. Fig. 5 compares TDMA and CDMA PER's with horizontal polarization. It should be noted that these systems require different bandwidths. Although the BER's for TDMA with $C_r = 3$ and CDMA with $C_r = 2$ and $N = 32$ were nearly identical, the PER's for the same situation differ significantly. In order to increase the performance of TDMA, one can use slow frequency hopping (Fig. 6). Within each platoon, a TDMA-type polling scheme is implemented. However, a different carrier frequency for each platoon is chosen, according to a pseudo-random hopping sequence, at the end of every packet reception. Thus, from Fig. 2, the cochannel interference power P_3 and P_4 are reduced since in any hop, there is a large probability that adjacent lanes use different carrier frequencies. For a reuse pattern $C_r = 2$, two independent sets of hopping frequencies (H) are used. A reuse factor of $C_r = 3$ and a set of $H = 10$ hopping frequencies outperform CDMA and TDMA schemes. Fig. 7 shows that

vertical polarization yields better results for distances less than 3 m, but slightly higher PER's for distances greater than 3 m.

C. Reliability and Spectrum Allocation

This section quantifies the different bandwidth requirements of the previous schemes by presenting numerical analysis results of reliability versus spectrum allocation. Reliability $R(T, d_g)$ is defined as the probability no message passes through our communication link in time T when the vehicles are at a distance d_g . Other sources also refer to this as the deadline failure probability. In our results, we have assumed a maximum "outage" time $T = 50$ ms at a link distance $d_g = 10$ m [4].

Although CDMA $C_r = 2$ and $N = 32$ gives better PER results than TDMA (Fig. 8), it requires much more bandwidth. Thus, we can implement TDMA by requiring very frequent transmissions, and although many of these transmissions would be lost, we are guaranteed a successful transmission using less bandwidth than CDMA. The gain in PER by frequency hopping also came as a result of greater bandwidth requirements, although not as much as CDMA. Interestingly, TDMA $C_r = 3$ requires less bandwidth for a given reliability than TDMA $C_r = 2$, since even though TDMA $C_r = 3$ requires more frequency bands per lane,

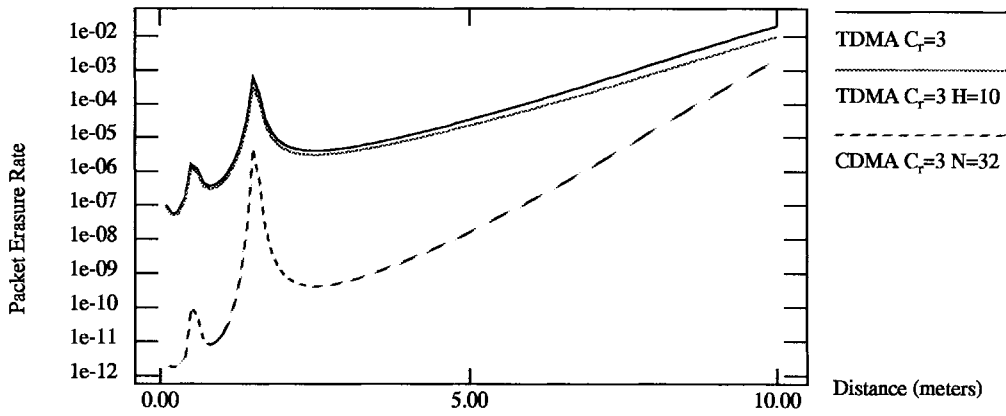


Fig. 5. Comparison of CDMA, TDMA, and slow-frequency hopping.

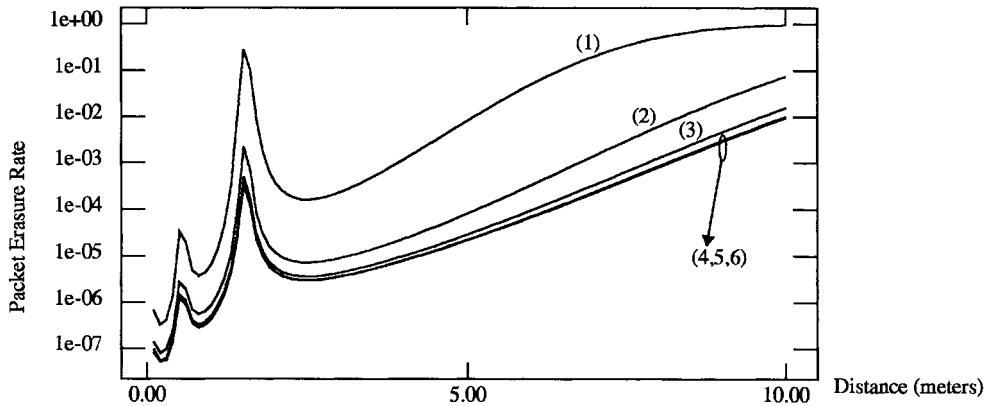


Fig. 6. TDMA with slow-frequency hopping for various reuse factors (C_r) and hopping frequencies (H): (1) $C_r = 1$ and $H = 10$, (2) $C_r = 1$ and $H = 100$, (3) $C_r = 2$ and $H = 10$, (4) $C_r = 2$ and $H = 100$, (5) $C_r = 3$ and $H = 10$, and (6) $C_r = 3$ and $H = 100$.

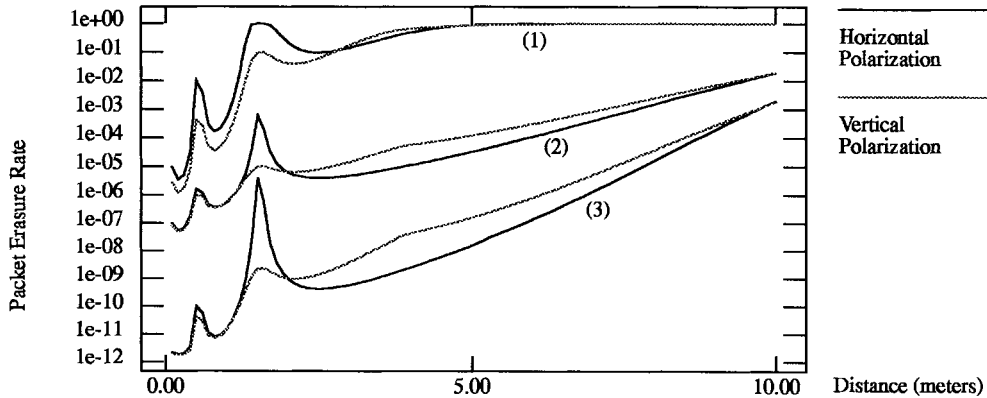


Fig. 7. Comparison of TDMA and CDMA PER's for horizontal and vertical polarization: (1) TDMA $C_r = 1$, (2) TDMA $C_r = 3$, and (3) CDMA $C_r = 2$ and $N = 32$.

the gain in PER is large enough that fewer transmissions are required. We see that for frequency hopping, this is not true.

D. Network Protocol

Section VI described a network protocol for TDMA transmissions. The concept of a complete cycle through a platoon was developed, and the idea propounded that the cycle sequence could be maintained without retransmission, even though the received code word differed from a valid code

word by more than the distance accepted for error correction. Again, employing the assumptions of the previous sections, it is shown how variations in M_1 (correcting distance used) and M_2 (error distance accepted for sync) affect the probability of cycle completion for both TDMA and frequency hopping.

Fig. 9 illustrates this. The probability of successful transmission between two links requires all links to have less than M_1 errors. The solid lines apply for only the link between the $n-1$ th and n th vehicle, which needs to have less than M_1 errors, while the $n-2$ prior links need only to have

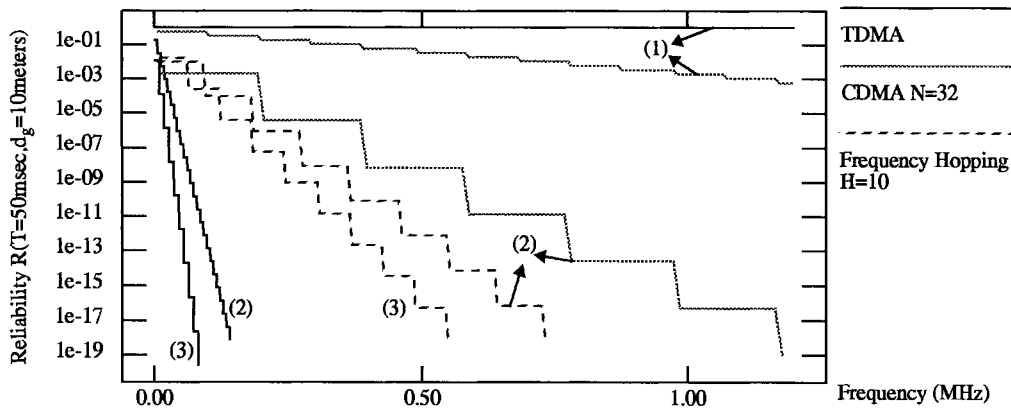


Fig. 8. Reliability versus spectrum allocation for CDMA, TDMA, and frequency hopping: (1) $C_r = 1$, (2) $C_r = 2$, and (3) $C_r = 3$.

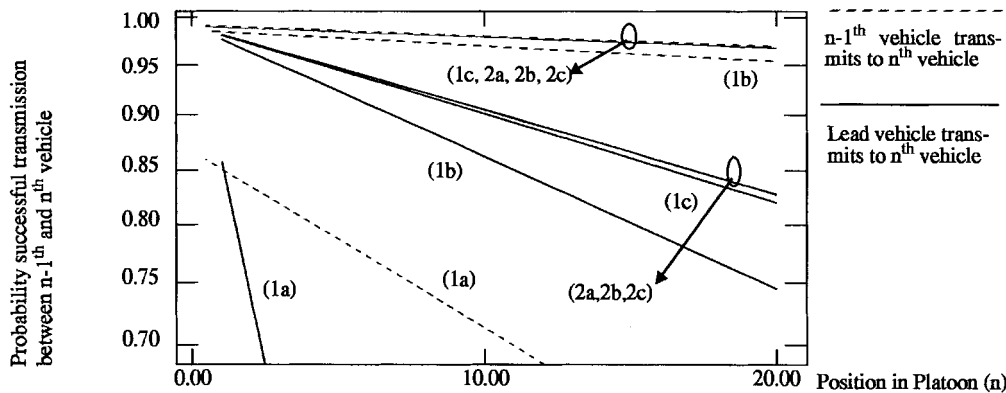


Fig. 9. Probability of one vehicle in platoon transmitting to another versus position in platoon. $M_1 = M_2 = 1$, $L = 76$, and $d_h = 10$ m: (1) $C = 3$ and (2) $C = 6$. (a) $H = 1$, (b) $H = 10$, and (c) $H = 100$.

less than M_2 errors. Thus, for TDMA, it is critical that a cycle be maintained, while for CDMA, where all vehicles transmit simultaneously, the preservation of the cycle is not so important.

VIII. CONCLUSIONS

We developed a statistical model for vehicle-to-vehicle radio channel applicable to AVCS communication, taking into account multipath reflections and a dominant wave, composed of a direct LOS wave with a strongly ground-reflected wave. The performance of this radio link was gauged by BER's, PER's, and deadline failure probability for a given bandwidth. These parameters were evaluated for three multiple-access techniques: TDMA, DS-CDMA, and TDMA within a platoon with frequency hopping outside the platoon.

Our analysis showed that deep fades and large probability of packet loss can occur for distances less than 3 m due to the cancellation of the ground-reflected wave and direct LOS wave. The effects of these fades could be reduced by employing vertical polarization as opposed to horizontal polarization. However, for a distance greater than 3 m, horizontal polarization PER and BER performance showed an improvement over vertical polarization. The performance difference between polarization techniques for distances greater than 3 m could be mitigated by decreasing cochannel interference (increasing the frequency reuse pattern, thus increasing bandwidth). Thus,

if frequency reuse between lanes is employed, vertical polarization can be implemented in order to mitigate the effects of deep fades caused by the destructive interference between the ground-reflected wave and direct LOS wave. Antenna diversity can also be used to increase performance, but was not considered here.

The system under study was also found to be sensitive to cochannel interference. Our analysis showed that even for CDMA transmission, performance could be largely improved if adjacent lanes use different frequencies. However, increasing the reuse factor greater than two, for CDMA, and three, for TDMA, did not afford better performance. According to our computations and within the validity of our assumptions, CDMA provides lower packet erasure probabilities than TDMA or slow frequency hopping. However, for a fixed bandwidth system, the reliability for a given bandwidth or delay-line failure probability appears to be better with TDMA. Here, we see a tradeoff between error probabilities and bandwidth. With CDMA, increased bandwidth results in lower error rates, however, with TDMA, even though the error rates may be greater than CDMA, many transmissions are possible since the bandwidth requirements of TDMA are minimal compared to CDMA. TDMA also affords the system designer to implement a protocol scheme in which correct packet reception is not necessary in order to transmit an update to the next vehicle. As our analysis showed, by varying the

allowable number of bit errors in a received packet, the delay in a TDMA system can be further reduced.

REFERENCES

- [1] K. Takada, Y. Tanaka, A. Igarashi, D. Fujita, "Road/automobile communication system and its economic effect," in *IEEE Vehicle Navigation and Information System Conf.*, 1989, pp. A15-21.
- [2] I. Catling and P. Belcher, "Autoguide-Route guidance in the United Kingdom," in *IEEE Vehicle Navigation and Information System Conf.*, 1989, pp. 467-473.
- [3] W. C. Collier and R. J. Weiland, "Smart cars, smart highways," *IEEE Spectrum*, vol. 34, pp. 27-33, Apr. 1994.
- [4] S. E. Shladover, C. A. Desoer, J. K. Hedrick, M. Tomizuka, J. Walrand, W. B. Zhang, D. H. McMahon, H. Peng, S. Sheikholeslam, and N. McKeown, "Automatic vehicle control developments in the PATH program," *IEEE Trans. Veh. Technol.*, vol. 40, no. 1, pp. 114-130, 1991.
- [5] W. C. Jakes, Ed., *Microwave Mobile Communication*. New York: Wiley, 1974.
- [6] R. H. Clarke, "A statistical theory of mobile radio reception," *Bell Syst. Tech. J.*, vol. 47, pp. 957-1000, July 1968.
- [7] A. S. Akki and F. Haber, "A statistical model of mobile to mobile land communication channel," *IEEE Trans. Veh. Technol.*, vol. 43, no. 1, pp. 2-7, 1986.
- [8] A. S. Akki, "Statistical properties of mobile-to-mobile land communication channels," *IEEE Trans. Veh. Technol.*, vol. 30, no. 4, pp. 826-831, 1994.
- [9] A. Hitchcock, "An example of quantitative evaluation of AVCS safety," in *Pacific Rim TransTech Conf. Proc.*, Seattle, WA, 1993, pp. 380-386.
- [10] J.-P. M. G. Linnartz and J. S. Davis, "Outage probability in digital cellular radio networks," in *Conf. Rec. of Asilomar Conf. on Signals, Systems, and Computers*, 1992, pp. 88-92.
- [11] H. Harley, "Short distance attenuation measurements at 900 MHz and 1.8 GHz using low antenna heights for microcells," *IEEE J. Select. Areas Commun.*, vol. 7, no. 1, pp. 5-10, 1989.
- [12] E. C. Jordan and K. G. Balmain, *Electromagnetic Waves and Radiating Systems*. New York: Prentice-Hall, 1968.
- [13] D. Parsons, *The Mobile Radio Propagation Channel*. New York: Wiley, 1992.
- [14] J. G. Proakis, *Digital Communications*, 2nd ed. New York: McGraw-Hill, 1989.
- [15] M. Abramowitz and I. A. Stegun, *Handbook of Mathematical Functions*. New York: Dover, 1974.
- [16] R. Diesta, C. O. U. Eleazu, and J.-P. M. G. Linnartz, "Packet-switched roadside base station to vehicle communication for intelligent vehicle/highway system," in *Proc. IEEE Veh. Technol. Conf. 1994*, pp. 401-404.
- [17] J.-P. M. G. Linnartz, *Narrowband Land-Mobile Radio Networks*. Boston, MA: Artech House, 1993.
- [18] T. Tank and J.-P. M. G. Linnartz, "Statistical characterization of Rician multipath effects in a mobile-to-mobile communication channel," *Int. J. Wireless Information Networks*, vol. 2, no. 1, pp. 17-26, Jan. 1995.
- [19] J.-P. M. G. Linnartz and J. Walrand, "Spectrum needs for IVHS," Calif. PATH Program Instit. Transport. Studies, Univ. Calif., Berkeley, CA, UCB Rep. ITS PWP-93-13, 1993.



Tushar Tank received the Bachelor of Science degree in electrical engineering in 1992 from Rutgers University, New Brunswick, NJ, and the Master's of Science degree in electrical engineering in 1994 from the University of California, Berkeley.

During his stay at Berkeley, he investigated various methods in modeling mobile telecommunication channels. From 1994 to 1995, he continued his research in digital communication as a Digital Signal Processing Engineer at Applied Signals Technology, Sunnyvale, CA. Currently, he is working on image processing at C-Cube Microsystems, Milpitas, CA. He has been investigating the field of digital communications and signal processing.



Jean-Paul M. G. Linnartz was born in Heerlen, the Netherlands, in 1961. He received the Ir. (M.Sc.E.E.) degree in electrical engineering (Cum Laude) from Eindhoven University of Technology, Eindhoven, the Netherlands, in 1986 and the Ph.D. degree (Cum Laude) in multiuser mobile radio nets from Delft University of Technology, Delft, the Netherlands, in 1991.

From 1987 to 1988, he worked with the Physics and Electronics Laboratory (F.E.L.-T.N.O., Hague) of the Netherlands Organization for Applied Scientific Research on frequency planning and UHF propagation. From 1988 to 1991, he was an Assistant Professor at Delft University of Technology. Since January 1992, he has been an Assistant Professor in the Department of E.E.C.S. at the University of California, Berkeley. In 1994, he returned to Delft University of Technology as an Associate Professor. Currently, he is with Philips Natuurkundig Laboratorium, Eindhoven. His main research interests are in (wireless) multimedia communications, conditional access and information security, electronic watermarks, intelligent vehicle highway systems, random access to fading channels, and multicarrier CDMA (combining OFDM and CDMA). In 1993, he published the book *Narrowband Land-Mobile Radio Networks*. He is the Editor of an interactive multimedia CD ROM on wireless communications.

Dr. Linnartz received the Dutch Veder Prize in 1991 for his research on teletraffic aspects in mobile radio networks.